Planar heterogeneous structures for coherent emission of radiation

C. J. Fu and Z. M. Zhang

G. W. Woodruff School of Mechanical Engineering, Georgia Institute of Technology, Atlanta, Georgia 30332

D. B. Tanner

Department of Physics, University of Florida, Gainesville, Florida 32611

Received January 14, 2005

The coupling of excited surface polaritons with thermal radiation through diffraction by gratings results in coherent thermal emission in a certain frequency range toward well-defined directions for p polarization. A planar coherent source is proposed that uses multilayers of negative permittivity (ϵ) and negative permeability (μ) materials. Owing to the excitation of surface polaritons at the interface between the negative-ϵ and negative-μ layers, coherent emission can be achieved for both s and p polarization. Moreover, one can control the emission frequency and direction by adjusting the layer thicknesses. © 2005 Optical Society of America

OCIS codes: 240.6690, 240.0310, 160.4760.

Nanotechnology has facilitated the manufacturing of materials and structures with unique optical properties. Many applications in optoelectronics, photonics, and energy conversion require accurate control of the emission spectrum and direction. A number of solutions to controlling the direction of emission of electromagnetic radiation have been proposed in recent years.[1–6] A coherent thermal emission source has been demonstrated that uses periodic structures to produce lobes of emitted radiation in well-defined directions.[1–3] However, the excited surface polaritons in the grating structure can couple with the emitted radiation for p polarization only.

In this Letter we describe a coherent emission source based on heterogeneous structures made from a layer of negative permittivity ϵ but positive permeability μ coupled with a layer of positive ϵ but negative μ. This bilayer structure is composed of what may be called single-negative materials,[7,8] in contrast to a metamaterial with simultaneous negative ϵ and μ (i.e., a negative refractive index).[9] The planar heterogeneous structure allows frequency-selective emission–absorption for both s and p polarization in well-defined directions. Many metals and polar dielectrics have a negative ϵ in the visible and infrared, and periodic structures of thin metal wires can dilute the average concentration of electrons and shift the plasma frequency to the far infrared or even into the gigahertz region.[10] Negative μ materials rarely exist in natural materials but can be obtained in the microwave region by use of metamaterials consisting of split-ring resonator elements.[11] Planar structures consisting of arrays of resonant elements have been fabricated and shown to exhibit a negative μ at terahertz frequencies and may be further scaled to higher frequencies.[12]

Consider a plane wave incident from vacuum onto a bilayer structure, shown in Fig. 1 (inset). For convenience, assume that medium 2 (thickness, d_2) is the layer with negative ϵ and that medium 3 is a thick (opaque) layer with negative μ and serves as the substrate of the layered structure. Spectral-directional emissivity $\epsilon_{\lambda,\theta}$ of the bilayer structure can be obtained from Kirchhoff's law[3]; thus $\epsilon_{\lambda,\theta}=1-R$, where R is the reflectance that can be calculated from the matrix formulation.[13] Assume that a plane wave of frequency ω is incident at an angle θ_1. The normal component of the wave vector in medium l ($l=1,2,3$) reads as $k_{lz}=(\epsilon_l\mu_l\omega^2/c^2-k_x^2)^{1/2}$, where c is the speed of light in vacuum and $k_x=\omega\sin\theta_1/c$ is the parallel component of the wave vector. Because ϵ and μ have opposite signs in media 2 and 3, k_{2z} and k_{3z} are purely imaginary when loss is neglected. A surface polariton can be excited at the interface of media 2 and 3 for s polarization when[14,15]

$$\frac{k_{2z}}{\mu_2}+\frac{k_{3z}}{\mu_3}=0 \tag{1}$$

and for p polarization when

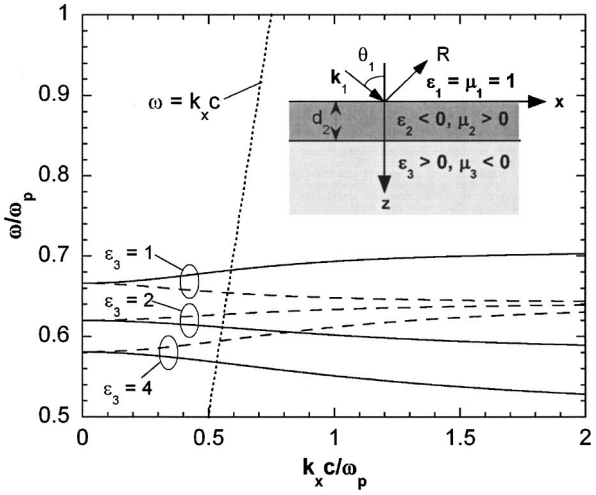

Fig. 1. Dispersion relations of surface polaritons at the interface of the two layers that make the bilayer (inset). Dashed lines, s polarization; solid lines, p polarization; dotted line, dispersion relation in vacuum.

0146-9592/05/141873-3/$15.00

$$\frac{k_{2z}}{\epsilon_2} + \frac{k_{3z}}{\epsilon_3} = 0. \tag{2}$$

In reality, dispersion and losses are inevitable. The following expressions are chosen to describe the electric and magnetic properties of the media[10,11]:

$$\epsilon_2(\omega) = 1 - \frac{{\omega_p}^2}{\omega^2 + i\gamma_e\omega}, \qquad \mu_2(\omega) = 1, \tag{3}$$

$$\mu_3(\omega) = 1 - \frac{F\omega^2}{\omega^2 - {\omega_0}^2 + i\gamma_m\omega}, \qquad \epsilon_3(\omega) = \epsilon_3, \tag{4}$$

where ω_p is the plasma frequency, ω_0 is the resonance frequency, γ_e and γ_m are the damping terms, and F is the fractional area of the unit cell occupied by the split ring. Although ϵ_3 is in general frequency dependent, for simplicity it will be taken as a real positive constant.

We calculate the dispersion relations of surface polaritons at the second interface by substituting Eqs. (3) and (4) into the expression for k_{lz} and Eqs. (1) and (2). The results in the lossless case ($\gamma_e = \gamma_m = 0$) are shown in Fig. 1 for different values of ϵ_3 with $\omega_0 = 0.5\omega_p$ and $F = 0.785$. The results are normalized with respect to ω_p. Surface polaritons can be excited for either polarization by both evanescent waves (within the region to the right of the dotted line) and propagating waves (within the region to the left of the dotted line) from vacuum. The dispersion curves give a nonzero ω for $k_x = 0$ ($\theta_1 = 0$), indicating that surface polaritons can be excited even at normal incidence. This behavior leads to some unique optical properties.

If both media 2 and 3 are lossless, R is always unity, because both k_{2z} and k_{3z} are purely imaginary and energy dissipation in the heterogeneous structure is zero. Therefore, loss must be included; in this case, the coupling between the surface polaritons and the electromagnetic wave enhances the absorption or emission at the polariton resonance frequencies. The corresponding emissivity $\epsilon_{\lambda,\theta}$ of the bilayer structure at 30° and 60° emission angles is plotted in Fig. 2 for s polarization with $\epsilon_3 = 4$, $\gamma_e = \gamma_m = 0.0025\omega_p$, and $d_2 = 0.425\lambda_p$ (where $\lambda_p = 2\pi c/\omega_p$). A very high $\epsilon_{\lambda,\theta}$ can be seen in a narrow frequency band centered at surface polariton resonance frequency $\omega_c = 0.584\omega_p$ for 30° and $0.592\omega_p$ for 60° emission angles. At frequencies outside the narrow band, $\epsilon_{\lambda,\theta}$ is nearly zero. Full width at half-maximum $\Delta\omega$ is approximately $0.007\omega_p$ for 30° and $0.005\omega_p$ for 60°; thus the corresponding Q ($=\omega_c/\Delta\omega$) factor is 85 and 120. In the inset of Fig. 2, $\epsilon_{\lambda,\theta}$ is plotted as a function of the angle of emission for fixed frequencies corresponding to $\omega_c = 0.584\omega_p$ and $\omega_c = 0.592\omega_p$. Angular emission lobes similar to those from a SiC grating[3] can be clearly seen. The angular emission lobes are relatively broad because of the relatively flat dispersion curves shown in Fig. 1 for small wave vector k_x. Similar results can be obtained for p polarization. Note that d_2 has a direct effect on the magnitude of $\epsilon_{\lambda,\theta}$ at center frequency ω_c and can be varied to optimize $\epsilon_{\lambda,\theta}$ for a given angle of emission. Parameters γ_e and γ_m were chosen to yield a small loss. Increasing loss will broaden the bandwidth and reduce the emission peak.

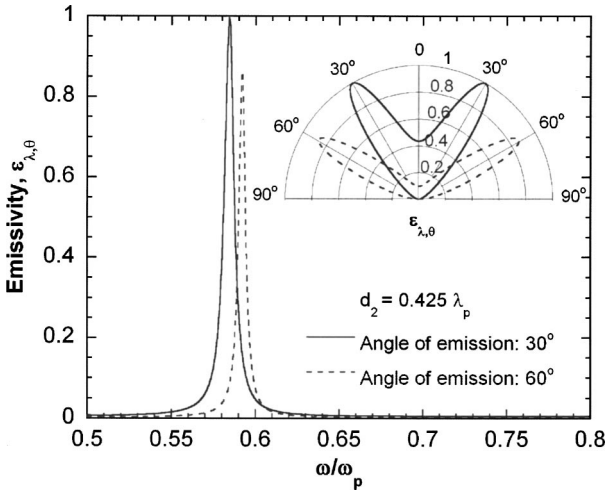

Fig. 2. Emissivity $\varepsilon_{\lambda,\theta}$ of the bilayer structure for s polarization versus ω/ω_p for 30° and 60° emission angles. Inset, the angular distribution for $\omega = 0.584\omega_p$ (solid curve) and $\omega = 0.592\omega_p$ (dashed curve).

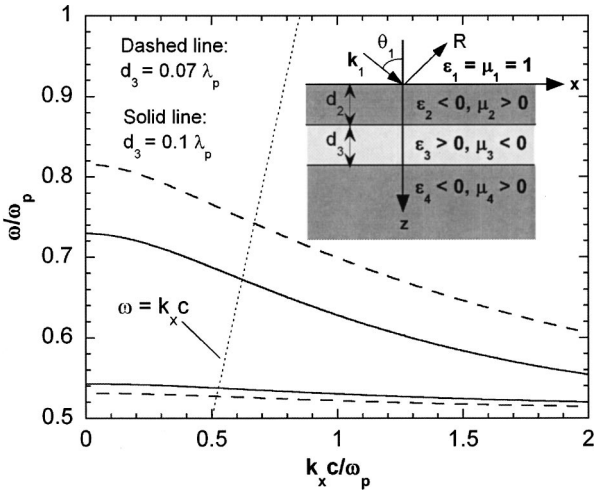

Fig. 3. Dispersion curves of a three-layer structure (inset), where the negative μ layer is sandwiched by two negative ε layers of the same material.

The frequency (wavelength) and direction of coherent emission from a grating can be varied by changing the grating period.[2,3] To tune the frequency and the emission angle, a modified structure is proposed, as shown in Fig. 3 (inset). Here, medium 1 is still a vacuum; medium 2 has thickness d_2 with $\epsilon_2 < 0$ and $\mu_2 > 0$; medium 3 has thickness d_3 with $\epsilon_3 > 0$ and $\mu_3 < 0$; and finally, the substrate (medium 4) is semi-infinite and is made from the same material as medium 2. In this structure, d_3 plays the key role in the control of the frequency and the angle of emission, because surface polaritons can be excited at both the second and the third interfaces. The excited surface polaritons will interact with each other if d_3 is small

enough. In that case, each dispersion curve shown in Fig. 1 splits into two curves. For p polarization, the dispersion relations are[15]

$$\frac{k_{2z}}{\epsilon_2} + \frac{k_{3z}}{\epsilon_3} \tanh\left(\frac{k_{3z}d_3}{2i}\right) = 0, \quad (5)$$

$$\frac{k_{2z}}{\epsilon_2} + \frac{k_{3z}}{\epsilon_3} \coth\left(\frac{k_{3z}d_3}{2i}\right) = 0. \quad (6)$$

The dispersion relations for s polarization are similar in form, with the exception that ϵ_2 and ϵ_3 are replaced with μ_2 and μ_3. Describing the material properties by Eqs. (3) and (4) and using $\epsilon_3 = 4$ yield the dispersion curves for p polarization calculated from Eqs. (5) and (6) that are shown in Fig. 3 for d_3 equal to $0.1\lambda_p$ (solid curves) and $0.07\lambda_p$ (dashed curves). The upper and lower branches of the curves correspond, respectively, to Eqs. (5) and (6). Comparing Fig. 3 with Fig. 1 clearly shows the splitting of the dispersion curve that is due to the reduced value of d_3. The upper branch has a much larger frequency shift than the lower branch, resulting in a steeper upper branch but a flatter lower branch. Therefore, coherent emission will be found at two different narrow frequency bands for each angle of emission. The emissivity of the three-layer heterogeneous structure is shown in Fig. 4 for a 30° emission angle. The value of d_2 is taken as $0.53\lambda_p$ such that large values of $\epsilon_{\lambda,\theta}$ appear around the higher surface polariton frequency, which is equal to $0.706\omega_p$ for $d_3 = 0.1\lambda_p$ and $0.782\omega_p$ for $d_3 = 0.07\lambda_p$. For a given emission direction, tuning the value of d_3 can control center frequency ω_c. The corresponding Q factor is 210 for $\omega_c = 0.706\omega_p$ and 175 for $\omega_c = 0.782\omega_p$. Finally, because the upper branch of the dispersion curves is so steep, very narrow angular emission lobes can be obtained using the trilayer heterogeneous structures, as shown in Fig. 4 (inset) for both $d_3 = 0.1\lambda_p$ and $d_3 = 0.07\lambda_p$ at their corresponding values of ω_c, as the curves overlap.

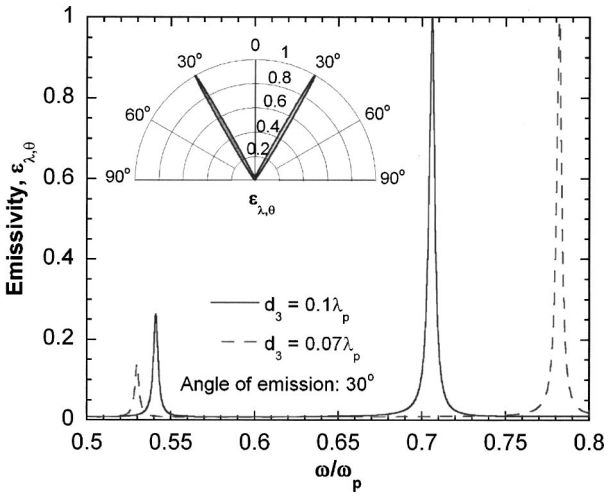

Fig. 4. Emissivity spectrum of the three-layer structure for p polarization at 30° emission angle with $d_2 = 0.53\lambda_p$ and two values of d_3. Inset, angular distribution for both $d_3 = 0.1\lambda_p$ and $d_3 = 0.07\lambda_p$ at their corresponding values of ω_c.

In summary, single-negative bilayer and trilayer heterogeneous structures may be used as coherent emission sources, working in both polarizations. To obtain coherent thermal emission, one must build the heterogeneous structures with the desired properties in the mid- and near-infrared regions.

This work was supported by the National Science Foundation (grants CTS-0082969 and CTS-0236831).
Z. M. Zhang's e-mail address is zhuomin.zhang@me.gatech.edu.

References

1. P. J. Hesketh, J. N. Zemel, and B. Gehart, Nature **325**, 549 (1986).
2. M. Kreiter, J. Oster, R. Sambles, S. Herminghaus, S. Mittler-Neher, and W. Knoll, Opt. Commun. **168**, 117 (1999).
3. J.-J. Greffet, R. Carminati, K. Joulain, J.-P. Mulet, S. Mainguy, and Y. Chen, Nature **416**, 61 (2002).
4. R. Biswas, E. Ozbay, B. Temelkuran, M. Bayindir, M. M. Sigalas, and K.-M. Ho, J. Opt. Soc. Am. B **18**, 1684 (2001).
5. S. Enoch, G. Tayeb, P. Sabouroux, N. Guérin, and P. Vincent, Phys. Rev. Lett. **89**, 213902 (2002).
6. P. Ben-Abdallah, J. Opt. Soc. Am. A **21**, 1368 (2004).
7. A. Alù and N. Engheta, IEEE Trans. Antennas Propag. **51**, 2558 (2003).
8. L.-G. Wang, H. Chen, and S.-Y. Zhu, Phys. Rev. B **70**, 245102 (2004).
9. R. A. Shelby, D. R. Smith, and S. Schultz, Science **292**, 77 (2001).
10. J. B. Pendry, A. J. Holden, W. J. Stewart, and I. Youngs, Phys. Rev. Lett. **76**, 4773 (1996).
11. J. B. Pendry, A. J. Holden, D. J. Rubbins, and W. J. Stewart, IEEE Trans. Microwave Theory Tech. **47**, 2075 (1999).
12. T. J. Yen, W. J. Padilla, N. Fang, D. C. Vier, D. R. Smith,J. B. Pendry, D. N. Basov, and X. Zhang, Science **303**, 1494 (2004).
13. Z. M. Zhang and C. J. Fu, Appl. Phys. Lett. **80**, 1097 (2002).
14. R. Rupin, Phys. Lett. A **277**, 61 (2000).
15. H. Raether, *Surface Plasmons on Smooth and Rough Surfaces and on Gratings* (Springer-Verlag, 1988), Chap. 2.